

**Christopher S. Lynch. "Strain Measurement."**

**Copyright 2000 CRC Press LLC. <<http://www.engnetbase.com>>.**

# Strain Measurement

---

Christopher S. Lynch

*The Georgia Institute of Technology*

- 22.1 Fundamental Definitions of Strain
- 22.2 Principles of Operation of Strain Sensors
  - Piezoresistive Foil Gages • Piezoresistive Semiconducting Gages • Piezoelectric Gages • Fiber Optic Strain Gages • Birefringent Film Strain Sensing • Moiré Strain Sensing

This chapter begins with a review of the fundamental definitions of strain and ways it can be measured. This is followed by a review of the many types of strain sensors and their application, and sources for strain sensors and signal conditioners. Next, a more detailed look is taken at operating principles of various strain measurement techniques and the associated signal conditioning.

## 22.1 Fundamental Definitions of Strain

---

Stress and strain are defined in many elementary textbooks about the mechanics of deformable bodies [1, 2]. The terms *stress* and *strain* are used to describe loads on and deformations of solid materials. The simplest types of solids to describe are homogeneous and isotropic. *Homogeneous* means the material properties are the same at different locations and *isotropic* means the material properties are independent of direction in the material. An annealed steel bar is homogeneous and isotropic, whereas a human femur is not homogeneous because the marrow has very different properties from the bone, and it is not isotropic because its properties are different along the length and along the cross-section.

The concepts of stress and strain are introduced in the context of a long homogeneous isotropic bar subjected to a tensile load (Figure 22.1). The stress  $\sigma$ , is the applied force  $F$  divided by the cross-sectional area  $A$ . The resulting strain  $\epsilon$ , is the length change  $\Delta L$ , divided by the initial length  $L$ . The bar elongates in the direction the force is pulling (longitudinal strain  $\epsilon_l$ ) and contracts in the direction perpendicular to the force (transverse strain  $\epsilon_t$ ).

When the strain is not too large, many solid materials behave like linear springs; that is, the displacement is proportional to the applied force. If the same force is applied to a thicker piece of material, the spring is stiffer and the displacement is smaller. This leads to a relation between force and displacement that depends on the dimensions of the material. Material properties, such as the density and specific heat, must be defined in a manner that is independent of the shape and size of the specimen. Elastic material properties are defined in terms of stress and strain. In the linear range of material response, the stress is proportional to the strain (Figure 22.2). The ratio of stress to strain for the bar under tension is an elastic constant called the Young's modulus  $E$ . The negative ratio of the transverse strain to longitudinal strain is the Poisson's ratio  $\nu$ .

Forces can be applied to a material in a manner that will cause distortion rather than elongation (Figure 22.3). A force applied tangent to a surface divided by the cross-sectional area is described as a shear stress  $\tau$ . The distortion can be measured by the angle change produced. This is the shear strain  $\gamma$

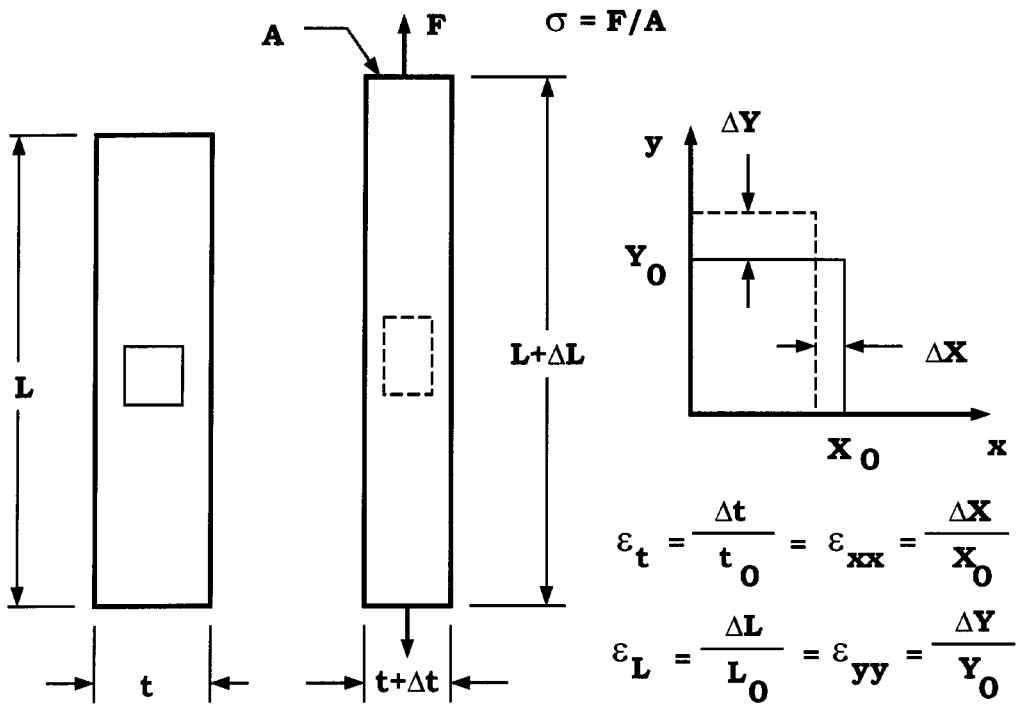


**FIGURE 22.1** When a homogeneous isotropic bar is stretched by a uniaxial force, it elongates in the direction of the force and contracts perpendicular to the force. The relative elongation and contraction are defined as the longitudinal and transverse strains, respectively.

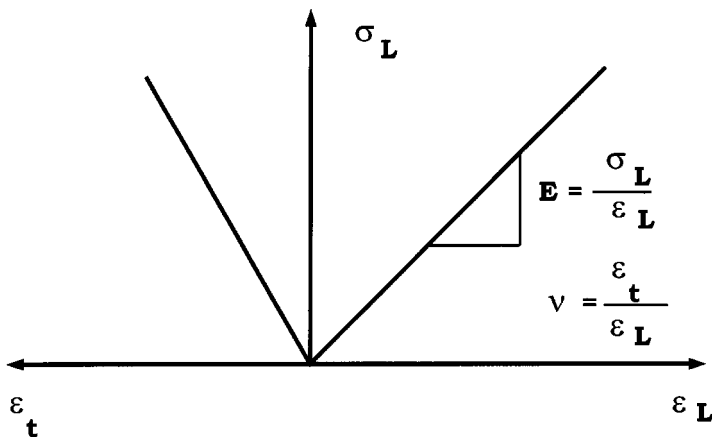


**FIGURE 22.2** The uniaxial force shown in Figure 22.1 produces uniaxial stress in the bar. When the material response is linear, the slope of the stress vs. strain curve is the Young's modulus. The negative ratio of the transverse to longitudinal strain is the Poisson's ratio.

when the angle change is small. When the relation between shear stress and shear strain is linear, the ratio of the shear stress to shear strain is the shear modulus  $G$ .

Temperature change also induces strain. This is thermal expansion. In most materials, thermal strain increases with temperature. Over a limited temperature range, the relationship between thermal strain

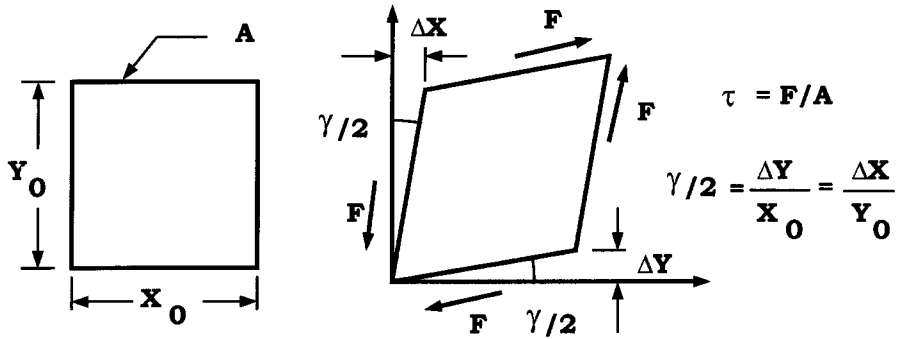


**FIGURE 22.3** When a block of material is subjected to forces parallel to the sides as shown, it distorts. The force per unit area is the shear stress  $\tau$ , and the angle change is the shear strain  $\gamma$ .

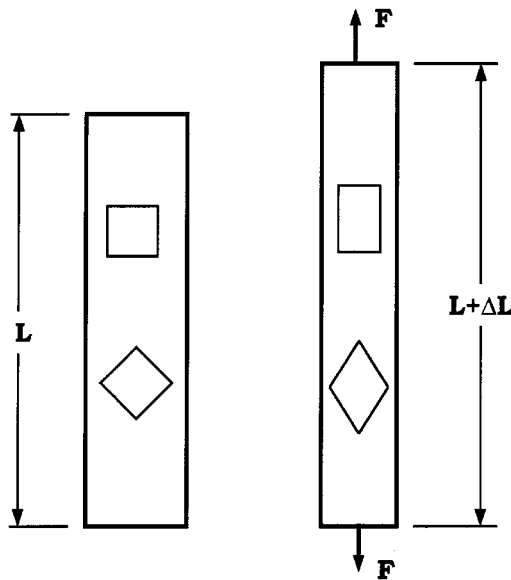


**FIGURE 22.4** Some elements of a bar under uniaxial tension undergo elongation and contraction. These elements lie in principal directions. Other elements undergo distortion as well.

and temperature is linear. In this case, the strain divided by the temperature change is the thermal expansion coefficient  $\alpha$ . In isotropic materials, thermal expansion only produces elongation strain, no shear strain.

Principal directions in a material are directions that undergo elongation but no shear. On any particular surface of a solid, there are always at least two principal directions in which the strain is purely elongation. This is seen if two squares are drawn on the bar under uniform tension (Figure 22.4). When the bar is stretched, the square aligned with the load is elongated, whereas the square at  $45^\circ$  is distorted (angles have changed) and elongated. If the principal directions are known, as with the bar under tension, then strain gages can be applied in these directions. If the principal directions are not known, such as near a hole or notch, in an anisotropic specimen, or in a structure with complicated geometry, then additional strain gages are needed to fully characterize the strain state.

The elastic and thermal properties can be combined to give Hooke's law, Equations 22.1 to 22.6.

$$\epsilon_{xx} = \frac{\sigma_{xx}}{E} - \frac{\nu}{E}(\sigma_{yy} + \sigma_{zz}) \quad (22.1)$$

$$\epsilon_{yy} = \frac{\sigma_{yy}}{E} - \frac{\nu}{E}(\sigma_{xx} + \sigma_{zz}) \quad (22.2)$$

$$\epsilon_{zz} = \frac{\sigma_{zz}}{E} - \frac{\nu}{E}(\sigma_{xx} + \sigma_{yy}) \quad (22.3)$$

$$\gamma_{xy} = \frac{\tau_{xy}}{G} \quad (22.4)$$

$$\gamma_{xz} = \frac{\tau_{xz}}{G} \quad (22.5)$$

$$\gamma_{yz} = \frac{\tau_{yz}}{G} \quad (22.6)$$

Several types of sensors are used to measure strain. These include piezoresistive gages (foil or wire strain gages and semiconductor strain gages), piezoelectric gages (polyvinylidene fluoride (PVDF) film and quartz), fiber optic gages, birefringent films and materials, and Moiré grids. Each type of sensor requires its own specialized signal conditioning. Selection of the best strain sensor for a given measurement is based on many factors, including specimen geometry, temperature, strain rate, frequency, magnitude, as well as cost, complexity, accuracy, spatial resolution, time resolution, sensitivity to transverse strain, sensitivity to temperature, and complexity of signal conditioning. [Table 22.1](#) describes typical characteristics of several sensors. [Table 22.2](#) lists some manufacturers and the approximate cost of the sensors and associated signal conditioning electronics.

The data in [Table 22.1](#) are to be taken as illustrative and by no means complete. The sensor description section describes only the type of sensor, not the many sizes and shapes. The longitudinal strain sensitivity is given as sensor output per unit longitudinal strain in the sensor direction. If the signal conditioning is included, the sensitivities can all be given in volts out per unit strain [3, 4], but this is a function of amplification and the quality of the signal conditioner. The temperature sensitivity is given as output change due to a temperature change. In many cases, higher strain resolution can be achieved, but resolving smaller strain is more difficult and may require vibration and thermal isolation. For the Moiré technique, the strain resolution is a function of the length of the viewing area. This technique can resolve a displacement of 100 nm (1/4 fringe order). This is divided by the viewing length to obtain the strain resolution. The spatial resolution corresponds to the gage length for most of the sensor types. The measurable strain range listed is the upper limit for the various sensors. Accuracy and reliability are usually reduced when sensors are used at the upper limit of their capability.

Manufacturers of the various sensors provide technical information that includes details of using the sensors, complete calibration or characterization data, and details of signal conditioning. The extensive technical notes and technical tips provided by Measurements Group, Inc. address such issues as thermal effects [5], transverse sensitivity corrections [6], soldering techniques [7], Rosettes [8], and gage fatigue [9]. Strain gage catalogs include information about gage materials, sizes, and selection. Manufacturers of other sensors provide similar information.

**TABLE 22.1** Comparison of Strain Sensors

Description	Longitudinal strain sensitivity	Transverse strain sensitivity	Temperature sensitivity	Strain resolution	Spatial resolution	Time resolution	Measurable strain range
Piezoresistive constantan foil	$\Delta R/R/\Delta \epsilon_L = 2.1$	$\Delta R/R/\Delta \epsilon_t = <0.02$	$\Delta R/R/\Delta T = 2 \times 10^{-6}/^\circ\text{C}$	$<1 \mu\text{strain}^a$	5–100 mm <sup>b</sup>	$<1 \mu\text{s}^c$	0–3%
Annealed constantan foil <sup>d</sup>	$\Delta R/R/\Delta \epsilon_L = 2.1$	$\Delta R/R/\Delta \epsilon_t = <0.02$	$\Delta R/R/\Delta T = 2 \times 10^{-6}/^\circ\text{C}$	$<11 \mu\text{strain}$	5–100 mm	$<1 \mu\text{s}$	0–10%
Piezoresistive semiconductor	$\Delta R/R/\Delta \epsilon_L = 150$	$\Delta R/R/\Delta \epsilon_t = ???$	$\Delta R/R/\Delta T = 1.7 \times 10^{-3}/^\circ\text{C}$	$<0.1 \mu\text{strain}$	1–15 mm	$<1 \mu\text{s}$	0–0.1%
Piezoelectric PVDF	$\Delta Q/A/\Delta \epsilon_L = 120 \text{ nC/m}^2/\mu\epsilon$	$\Delta Q/A/\Delta \epsilon_t = 60 \text{ nC/m}^2/\mu\epsilon$	$\Delta Q/A/\Delta T = -27 \mu\text{C/m}^2/^\circ\text{C}$	1–10 $\mu\text{strain}$	Gage size	$<1 \mu\text{s}$	0–30%
Piezoelectric quartz	$\Delta Q/A/\Delta \epsilon_L = 150 \text{ nC/m}^2/\mu\epsilon$ bonded to steel		$\Delta Q/A/\Delta T = 0$	$<0.01 \mu\text{strain}$ 20 mm gage	Gage size	$<10 \mu\text{s}$	0–0.1%
Fiber optic Fabry–Perot	2 to 1000 $\mu\text{strain}/\text{V}$	Near zero		$<1 \mu\text{strain}$	2–10 mm	$<20 \mu\text{s}$	
Birefringent Film	$K^e = 0.15\text{--}0.002$				0.5 mm <sup>f</sup>	$<5 \mu\text{s}$	0.05–5%
Moiré	1 fringe order/417 nm displ.	1 fringe order/417 nm displ.	Not defined	41.7 $\mu\epsilon$ over 10 mm	full field <sup>g</sup>	Limited by signal conditioning	0.005–5%

<sup>a</sup> With good signal conditioning.

<sup>b</sup> Equal to grid area.

<sup>c</sup> Gage response is within 100 ns. Most signal conditioning limits response time to far less than this.

<sup>d</sup> Annealed foil has a low yield stress and a large strain to failure. It also has hysteresis in the unload and a zero shift under cyclic load.

<sup>e</sup> This technique measures a difference in principal strains.  $\epsilon_2 - \epsilon_1 = N\lambda/2tK$

<sup>f</sup> Approximately the film thickness.

<sup>g</sup> The spatial strain resolution depends on the strain level. This is a displacement measurement technique.

**TABLE 22.2** Sources and Prices of Strain Sensors

Supplier	Address	Sensor Types	Sensor Cost	Signal Conditioning	Cost
Micro Measurements	P.O. Box 27777 Raleigh, NC 27611	Piezoresistive foil Birefringent film	From \$5.00 From \$10.00	Wheatstone bridge Polariscope	From \$500 \$5000 to 10,000
Texas Measurements	P.O. Box 2618 College Station, TX 77841	Piezoresistive foil and wire Load cells	From \$5.00		
Omega Engineering	P.O. Box 4047 Stamford, CT 06907-0047	Piezoresistive foil	From \$5.00	Strain meter Wheatstone bridge	From \$550 From \$2700
Dynasen, Inc.	20 Arnold Pl. Goleta, CA 93117	Piezoresistive foil Specialty gages for shock wave measurements Piezoelectric PVDF (calibrated)	From \$55.00 From \$55.00	2-Channel pulsed Wheatstone bridge Passive charge integrator	\$5000 \$250.00
Entran Sensors and Electronics	Entran Devices, Inc. 10 Washington Ave. Fairfield, NJ 07004-3877	Piezoresistive semiconductor	From \$15.00		
Amp Inc.	Piezo Film Sensors P.O. Box 799 Valley Forge, PA 19482	Piezoelectric PVDF (not calibrated)	From \$5.00		
Kistler Instrument Corp.	Amherst, NY 14228-2171	Piezoelectric quartz		Electrometer Charge amplifier Electronics	
F&S Inc.	Fiber and Sensor Technologies P.O. Box 11704, Blacksburg, VA 24062-1704	Fabry–Perot strain sensors	From \$75		From \$3500.00
Photomechanics, Inc.	512 Princeton Dr. Vestal, NY 13850-2912	Moiré interferometer			\$60,000

## 22.2 Principles of Operation of Strain Sensors

### Piezoresistive Foil Gages

Piezoresistive foil and wire gages comprise a thin insulating substrate (usually polyimide film), a foil or wire grid (usually constantan) bonded to the substrate, lead wires to connect the grid to a resistance measuring circuit, and often an insulating encapsulation (another sheet of polyimide film) (Figure 22.5). The grid is laid out in a single direction so that strain will stretch the legs of the grid in the length direction. The gages are designed so that strain in the width or transverse direction separates the legs of the grid without straining them. This makes the gage sensitive to strain only along its length. There is always some sensitivity to transverse strain, and almost no sensitivity to shear strain. In most cases, the transverse sensitivity can be neglected.

When piezoresistive foil or wire strain gages are bonded to a specimen and the specimen is strained, the gage strains as well. The resistance change is related to the strain by a gage factor, Equation 22.7.

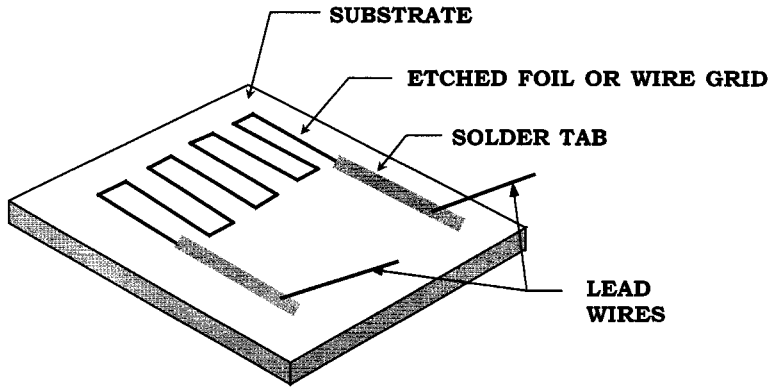


FIGURE 22.5 Gage construction of a foil or wire piezoresistive gage.

$$\frac{\Delta R}{R} = G_L \epsilon_L \quad (22.7)$$

where  $\Delta R/R$  = Relative resistance change

$G$  = Gage factor

$\epsilon$  = Strain

These gages respond to the average strain over the area covered by the grid [10]. The resistance change is also sensitive to temperature. If the temperature changes during the measurement period, a correction must be made to distinguish the strain response from the thermal response. The gage response to longitudinal strain, transverse strain, and temperature change is given by Equation 22.8.

$$\frac{\Delta R}{R} = G_L \epsilon_L + G_t \epsilon_t + G_T \Delta T \quad (22.8)$$

where  $G_L$ ,  $G_t$ , and  $G_T$  are the longitudinal, transverse, and temperature sensitivity, respectively. Micromeritics, Inc. uses a different notation. Their gage data is provided as  $G_L = F_G$ ,  $G_t = K_t F_G$ ,  $G_T = \beta_g$ . When a strain gage is bonded to a specimen and the temperature changes, the strain used in Equation 22.8 is the total strain, thermal plus stress induced, as given by Equation 22.7.

The temperature contribution to gage output must be removed if the gages are used in tests where the temperature changes. A scheme referred to as self-temperature compensation (STC) can be used. This is accomplished by selecting a piezoresistive material whose thermal output can be canceled by the strain induced by thermal expansion of the test specimen. Gage manufacturers specify STC numbers that match the thermal expansion coefficients of common specimen materials.

Strain of piezoresistive materials produces a relative resistance change. The resistance change is the result of changes in resistivity and dimensional changes. Consider a single leg of the grid of a strain gage with a rectangular cross-section (Figure 22.6). The resistance is given by Equation 22.9.

$$R = \rho \frac{L}{A} \quad (22.9)$$

where  $R$  = Resistance

$\rho$  = Resistivity

$L$  = Length

$A$  = Area of the cross-section



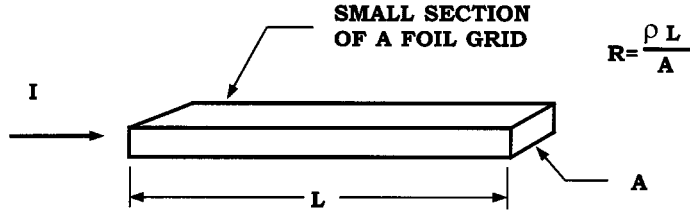


**FIGURE 22.6** A single leg of a piezoresistive gage is used to explain the source of the relative resistance change that occurs in response to strain.

A small change in resistance is given by the first-order terms of a Taylor's series expansion, Equation 22.10.

$$\Delta R = \frac{\partial R}{\partial \rho} \Delta \rho + \frac{\partial R}{\partial L} \Delta L + \frac{\partial R}{\partial A} \Delta A \quad (22.10)$$

Differentiating Equation 22.9 to obtain each term of Equation 22.10 and then dividing by the initial resistance leads to Equation 22.11.

$$\frac{\Delta R}{R_0} = \frac{\Delta \rho}{\rho_0} + \frac{\Delta L}{L_0} - \frac{\Delta A}{A_0} \quad (22.11)$$

The relative resistance change is due to a change in resistivity, a change in length strain, and a change in area strain.

The strain gage is a composite material. The metal in a strain gage is like a metal fiber in a polymer matrix. When the polymer matrix is deformed, the metal is dragged along in the length direction; but in the width and thickness directions, the strain is not passed to the metal. This results in a stress state called uniaxial stress. This state was discussed in the examples above. The mathematical details involve an inclusion problem [11, 12]. Accepting that the stress state is uniaxial, the relationship between the area change and the length change in Equation 22.11 is found from the Poisson's ratio. The area strain is the sum of the width and thickness strain, Equation 22.12.

$$\frac{\Delta A}{A_0} = \frac{\Delta w}{w_0} + \frac{\Delta t}{t_0} \quad (22.12)$$

The definition of the Poisson's ratio gives Equation 22.13.

$$\frac{\Delta A}{A_0} = -2\nu \frac{\Delta L}{L_0} \quad (22.13)$$

where  $\Delta w/w =$  width strain and  $\Delta t/t =$  thickness strain. Substitution of Equation 22.13 into Equation 22.11 gives Equation 22.14 for the relative resistance change.

$$\frac{\Delta R}{R_0} = \frac{\Delta \rho}{\rho_0} + \frac{\Delta L}{L_0} (1 + 2\nu) \quad (22.14)$$

The relative resistivity changes in response to stress. The resistivity is a second-order tensor [13], and the contribution to the overall resistance change can be found in terms of strain using the elastic

constitutive law [14]. The results lead to an elastic gage factor just over 2 for constantan gages. If the strain is large, the foil or wire in the gage will experience plastic deformation. When the deformation is plastic, the resistivity change is negligible and the dimensional change dominates. In this case, Poisson's ratio is 0.5 and the gage factor is 2. This effect is utilized in manufacturing gages for measuring strains larger than 1.5%. In this case, annealed foil is used. The annealed foil undergoes plastic deformation without failure. These gages are capable of measuring strain in excess of 10%. When metals undergo plastic deformation, they do not unload to the initial strain. This shows up as hysteresis in the gage response, that is, on unload, the resistance does not return to its initial value.

Foil and wire strain gages can be obtained in several configurations. They can be constructed with different backing materials, and left open faced or fully encapsulated. Backing materials include polyimide and glass fiber-reinforced phenolic resin. Gages can be obtained with solder tabs for attaching lead wires, or with lead wires attached. They come in many sizes, and in multiple gage configurations called rosettes.

Strain gages are mounted to test specimens with adhesives using a procedure that is suitable for bonding most types of strain sensors. This is accomplished in a step-by-step procedure [15] that starts with surface preparation. An overview of the procedure is briefly described. To successfully mount strain gages, the surface is first degreased. The surface is abraded with a fine emery cloth or 400 grit paper to remove any loose paint, rust, or deposits. Gage layout lines are drawn (not scribed) on the surface in a cross pattern with pen or pencil, one line in the grid direction and one in the transverse direction. The surface is then cleaned with isopropyl alcohol. This can be done with an ultrasonic cleaner or with wipes. If wiped, the paper or gauze wipe should be folded and a small amount of alcohol applied. The surface should be wiped with one pass and the wipe discarded. This should be repeated, wiping in the other direction. The final step is to neutralize the surface, bringing the alkalinity to a pH of 7 to 7.5. A surface neutralizer is available from most adhesive suppliers. The final step is to apply the gage.

Gage application is accomplished with cellophane tape, quick-set glue, and a catalyst. The gage is placed on a clean glass or plastic surface with bonding side down, using tweezers. (Never touch the gage. Oils from skin prevent proper adhesion.) The gage is then taped down with a 100 mm piece of cellophane tape. The tape is then peeled up with the gage attached. The gage can now be taped onto its desired location on the test specimen. Once the gage has been properly aligned, the tape is peeled back from one side, lifting the gage from the surface. The tape should remain adhered to the surface about 1 cm from the gage. Note that one side of the tape is still attached to the specimen so that the gage can be easily returned to its desired position. A thin coating of catalyst is applied to the exposed gage surface. A drop of glue is placed at the joint of the tape and the specimen. Holding the tape at about a 30° angle from the surface, the tape can be slowly wiped down onto the surface. This moves the glue line forward. After the glue line has passed the gage, the gage should be pressed in place and held for approximately 1 min. The tape can now be peeled back to expose the gage, and lead wires can be attached.

The relative resistance change of piezoresistive gages is usually measured using a Wheatstone bridge [16]. This allows a small change of resistance to be measured relative to an initial zero value, rather than relative to a large resistance value, with a corresponding increase in sensitivity and resolution. The Wheatstone bridge is a combination of four resistors and a voltage source (Figure 22.7). One to four of the resistors in the bridge can be strain gages. The output of the bridge is the difference between the voltage at points B and D. Paths ABC and ADC are voltage dividers so that  $V_B$  and  $V_D$  are given by Equations 22.15a and b.

$$V_B = V_{in} \frac{R_2}{R_1 + R_2} \quad (22.15a)$$

$$V_D = V_{in} \frac{R_3}{R_3 + R_4} \quad (22.15b)$$

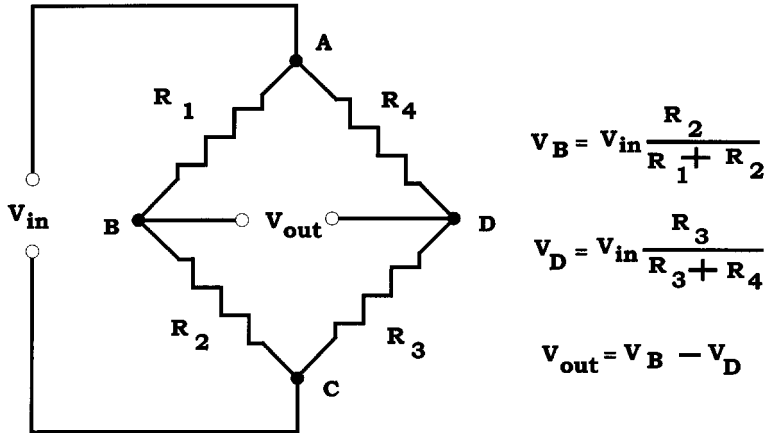


FIGURE 22.7 The Wheatstone bridge is used to measure the relative resistance change of piezoresistive strain gages.

The bridge output, Equation 22.16, is zero when the balance condition, Equation 22.17, is met.

$$V_0 = V_B - V_D \quad (22.16)$$

$$R_1 R_3 = R_2 R_4 \quad (22.17)$$

Wheatstone bridge signal conditioners are constructed with a way to “balance” the bridge by adjusting the ratio of the resistances so that the bridge output is initially zero.

The balance condition is no longer met if the resistance values undergo small changes  $\Delta R_1$ ,  $\Delta R_2$ ,  $\Delta R_3$ ,  $\Delta R_4$ . If the values  $R_1 + \Delta R_1$ , etc. are substituted into Equation 22.15, the results substituted into Equation 22.16, condition (22.17) used, and the higher order terms neglected, the result is Equation 22.18 for the bridge output.

$$V_{out} = V_{in} \frac{R_1 R_3}{(R_1 + R_2)(R_3 + R_4)} \left( -\frac{\Delta R_1}{R_1} + \frac{\Delta R_2}{R_2} - \frac{\Delta R_3}{R_3} + \frac{\Delta R_4}{R_4} \right) \quad (22.18)$$

The Wheatstone bridge can be used to directly cancel the effect of thermal drift. If  $R_1$  is a strain gage bonded to a specimen and  $R_2$  is a strain gage held onto a specimen with heat sink compound (a thermally conductive grease available at any electronics store), then  $R_1$  will respond to strain plus temperature, and  $R_2$  will only respond to temperature. Since the bridge subtracts the output of  $R_1$  from that of  $R_2$ , the temperature effect cancels.

The sensitivity of a measuring system is the output per unit change in the quantity to be measured. If the resistance change is from a strain gage, the sensitivity of the Wheatstone bridge system is proportional to the input voltage. Increasing the voltage increases the sensitivity. There is a practical limitation to increasing the voltage to large values. The power dissipated (heat) in the gage is  $P = I^2 R$ , where  $I$ , the current through the gage, can be found from the input voltage and the bridge resistances. This heat must go somewhere or the temperature of the gage will continuously rise and the resistance will change due to heating. If the gage is mounted on a good thermal conductor, more power can be conducted away than if the gage is mounted on an insulator. The specimen must act as a heat sink.

Heat sinking ability is proportional to the thermal conductivity of the specimen material. A reasonable temperature gradient to allow the gage to induce in a material is 40°C per meter (about 1°C per 25 mm).

For thick specimens (thickness several times the largest gage dimension), this can be conducted away to the grips or convected to the surrounding atmosphere. If the four bridge resistances are approximately equal, the power to the gage in terms of the bridge voltage is given by Equation 22.19.

$$P_g = \frac{V_{in}^2}{4R} \quad (22.19)$$

The power per unit grid area,  $A_g$ , or power density to the gage can be equated to the thermal conductivity of the specimen and the allowable temperature gradient in the specimen by Equation 22.20.

$$\frac{P_g}{A_g} = \frac{V_{in}^2}{4RA_g} = K\nabla T \quad (22.20)$$

Thermal conductivities of most materials can be found in tables or on the Web. Some typical values are Al:  $K = 204 \text{ W m}^{-1} \text{ }^\circ\text{C}^{-1}$ , steel:  $K = 20 \text{ to } 70 \text{ W m}^{-1} \text{ }^\circ\text{C}^{-1}$ , glass:  $K = 0.78 \text{ W m}^{-1} \text{ }^\circ\text{C}^{-1}$  [17].

The acceptable bridge voltage can be calculated from Equation 22.21.

$$V_{in} = \sqrt{K\nabla T 4RA_g} \quad (22.21)$$

A sample calculation shows that for a  $0.010 \text{ m} \times 0.010 \text{ m}$   $120 \text{ } \Omega$  grid bonded to a thick piece of aluminum with a thermal conductivity of  $204 \text{ W m}^{-1} \text{ }^\circ\text{C}^{-1}$  and an acceptable temperature gradient of  $40^\circ\text{C}$  per meter, the maximum bridge voltage is  $19 \text{ V}$ . If thin specimens are used, the allowable temperature gradient will be smaller. If smaller gages are used for better spatial resolution, the bridge excitation voltage must be reduced with a corresponding reduction in sensitivity.

A considerably higher bridge voltage can be used if the bridge voltage is pulsed for a short duration. This dissipates substantially less energy in the gage and thus increases the sensitivity by a factor of 10 to 100. Wheatstone bridge pulse power supplies with variable pulse width from  $10 \text{ } \mu\text{s}$  and excitation of  $350 \text{ V}$  are commercially available [18].

The strain measurement required is often in a complex loading situation where the directions of principal strain are not known. In this case, three strain gages must be bonded to the test specimen at three angles. This is called a strain rosette. The angle between the rosette and the principal directions, as well as the magnitude of the principal strains, can be determined from the output of the rosette gages. This is most easily accomplished using the construct of a Mohr's circle (Figure 22.8).

A common rosette is the  $0\text{--}45\text{--}90^\circ$  pattern. The rosette is bonded to the specimen with relative rotations of  $0^\circ$ ,  $45^\circ$ , and  $90^\circ$ . These will be referred to as the  $x$ ,  $x'$ , and  $y$  directions. The principal directions are labeled the 1 and 2 directions. The unknown angle between the  $x$  direction and the 1 direction is labeled  $\theta$ . The Mohr's circle is drawn with the elongational strain on the horizontal axis and the shear strain on the vertical axis. The center of the circle is labeled  $C$  and the radius  $R$ . The principal directions correspond to zero shear strain. The principal values are given by Equations 22.22 and 22.23.

$$\epsilon_1 = C + R \quad (22.22)$$

$$\epsilon_2 = C - R \quad (22.23)$$

A rotation through an angle  $2\theta$  on the Mohr's circle corresponds to a rotation of the rosette of  $\theta$  relative to the principal directions. The center of the circle is given by Equation 22.24 and the output of the strain gages is given by Equations 22.25 to 22.27.

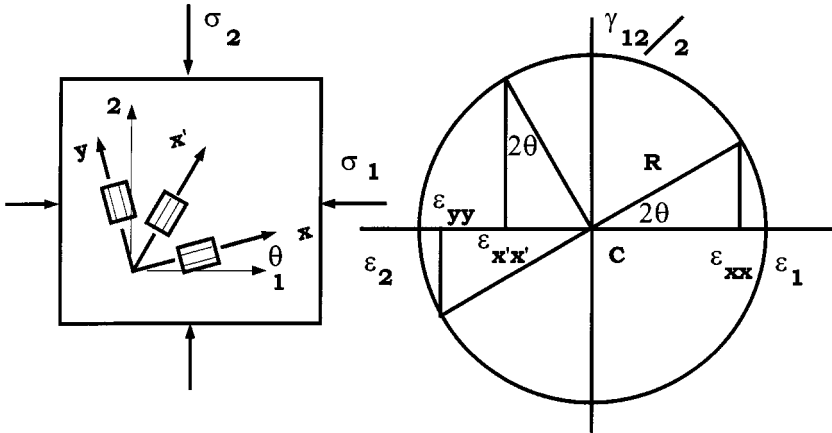


**FIGURE 22.8** A three-element rosette is used to measure strain when the principal directions are not known. The Mohr's circle is used to find the principal directions and the principal strain values.

$$C = \frac{\epsilon_{xx} + \epsilon_{yy}}{2} \quad (22.24)$$

$$\epsilon_{xx} - C = R \cos 2\theta \quad (22.25)$$

$$\epsilon_{x'x'} - C = -R \sin 2\theta \quad (22.26)$$

$$\epsilon_{yy} - C = -R \cos 2\theta \quad (22.27)$$

Dividing Equation 22.25 by Equation 22.26 leads to  $\theta$  and then to  $R$ , Equations 22.28 and 22.29.

$$R^2 = (\epsilon_{xx} - C)^2 + (\epsilon_{x'x'} - C)^2 \quad (22.28)$$

$$\tan 2\theta = \frac{C - \epsilon_{x'x'}}{\epsilon_{xx} - C} \quad (22.29)$$

The principal directions and principal strain values have been found from the output of the three rosette gages.

## Piezoresistive Semiconducting Gages

Piezoresistive semiconductor strain gages, like piezoresistive foil and wire gages, undergo a resistance change in response to strain, but with nearly an order of magnitude larger gage factor [19]. The coupling between resistance change and temperature is very large, so these gages have to be temperature compensated. The change of resistance with a small temperature change can be an order of magnitude larger than that induced by strain. Semiconductor strain gages are typically used to manufacture transducers such as load cells. They are fragile and require great care in their application.

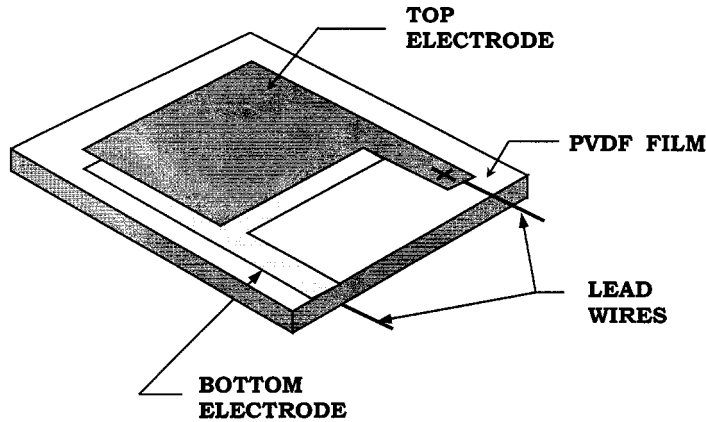


FIGURE 22.9 Typical gage construction of a piezoelectric gage.

## Piezoelectric Gages

Piezoelectric strain gages are, effectively, parallel plate capacitors whose dielectric changes polarization in response to strain [14]. When the polarization changes, a charge proportional to the strain is produced on the electrodes. PVDF film strain gages are inexpensive, but not very accurate and subject to depoling by moderate temperature. They make good sensors for dynamic measurements such as frequency and logarithm decrement, but not for quantitative measurements of strain. When used for quasistatic measurements, the charge tends to drain through the measuring instrument. This causes the signal to decay with a time constant dependent on the input impedance of the measuring instrument. Quartz gages are very accurate, but also lose charge through the measuring instrument. Time constants can be relatively long (seconds to hours) with electrometers or charge amplifiers.

The PVDF gage consists of a thin piezoelectric film with metal electrodes (Figure 22.9). Lead wires connect the electrodes to a charge measuring circuit. Gages can be obtained with the electrodes encapsulated between insulating layers of polyimide.

The gage output can be described in terms of a net dipole moment per unit volume. If the net dipole moment is the total charge,  $Q$ , on the electrodes multiplied by spacing,  $d$ , between the electrodes, then the polarization is given by Equation 22.30.

$$P = \frac{Qd}{V} \quad (22.30)$$

From Equation 22.30, it is seen that the polarization  $P$  (approximately equal to the electric displacement  $D$ ) is the charge per unit electrode area (Figure 22.10).

A Taylor's series expansion of Equation 22.30 gives Equation 22.31.

$$\Delta P = \frac{\partial P}{\partial V} \Delta V + \frac{\partial P}{\partial(Qd)} \Delta Qd \quad (22.31)$$

Which, after differentiating Equation 22.30 and substituting becomes Equation 22.31.

$$\Delta P = \frac{\Delta Qd}{V_0} - \frac{\Delta V}{V_0} P_0 \quad (22.32)$$

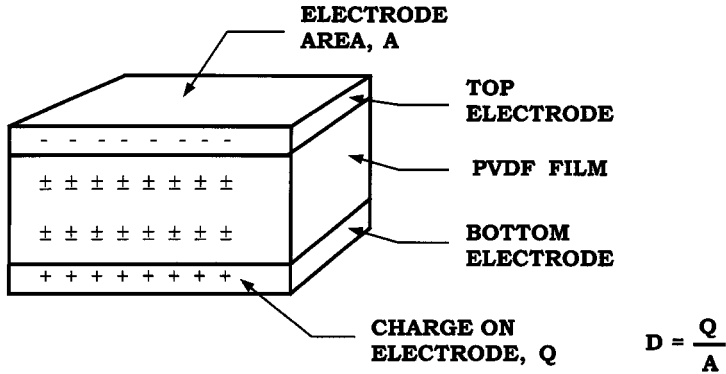


**FIGURE 22.10** A representative cross-section of a piezoelectric material formed into a parallel plate capacitor. The piezoelectric material is polarized. This results in a charge on the electrodes. When the material is strained, the polarization changes and charge flows.

For PVDF film, the second term in Equation 22.32 dominates. The output is proportional to the remanent polarization  $P_0$ . The remanent polarization slowly decays with time, has a strong dependence on temperature, and decays rapidly at temperatures around 50°C. This makes accuracy a problem. If the sensors are kept at low temperature, accuracy can be maintained within  $\pm 3\%$ .

Strain sensors can also be constructed from piezoelectric ceramics like lead zirconate titanate (PZT) or barium titanate. Ceramics are brittle and can be depoled by strain so should only be used at strains less than 200 microstrain. PZT loses some of its polarization with time and thus has accuracy problems, but remains polar to temperatures of 150°C or higher. “Hard” PZT (usually iron doped) is the best composition for polarization stability and low hysteresis. Quartz has the best accuracy. It is not polar, but polarization is induced by strain. Quartz has excellent resolution and accuracy over a broad temperature range but is limited to low strain levels. It is also brittle, so is limited to small strain.

Two circuits are commonly used for piezoelectric signal conditioning: the electrometer and the charge amplifier (Figure 22.11). In the electrometer circuit, the piezoelectric sensor is connected to a capacitor with a capacitance value  $C$ , at least 1000 times that of the sensor  $C_g$ . There is always some resistance in

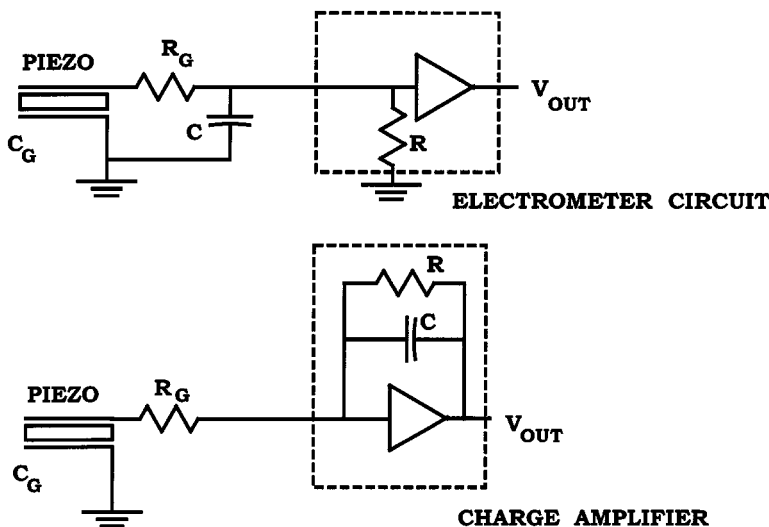


**FIGURE 22.11** The electrometer and charge amplifier are the most common circuits used to measure charge from piezoelectric transducers.

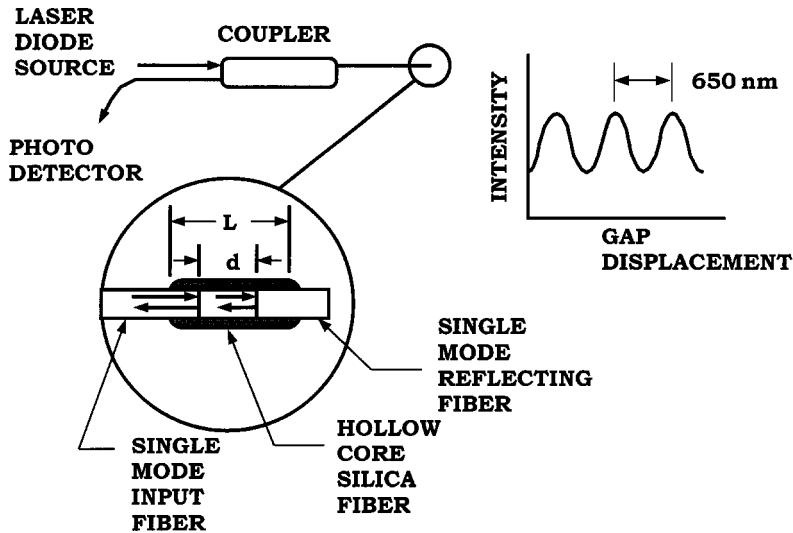


FIGURE 22.12 A schematic of the Fabry–Perot fiber optic strain gage. When the cavity elongates, alternating constructive and destructive interference occur.

the cable that connects the sensor to the capacitor. The circuit is simply two capacitors in parallel connected by a resistance. The charge equilibrates with a time constant given by  $R_g C_g$ . This time constant limits the fastest risetime that can be resolved to about 50 ns, effectively instantaneous for most applications. The charge is measured by measuring the voltage on the capacitor, then using Equation 22.33.

$$Q = CV \tag{22.33}$$

The difficulty is that measuring devices drain the charge, causing a time decay with a time constant  $RC$ . This causes the signal to be lost rapidly if conventional op amps are used. FET input op amps have a very high input impedance and can extend this time constant to many hours. The charge amplifier is another circuit used to measure charge. This is usually an FET input op amp with a capacitor feedback. This does not really amplify charge, but produces a voltage proportional to the input charge. Again, the time constant can be many hours, allowing use of piezoelectric sensors for near static measurements.

High input impedance electrometer and charge amplifier signal conditioners for near static measurements are commercially available [20] as well as low-cost capacitive terminators for high-frequency (high kilohertz to megahertz) measurements [18]. An advantage of piezoelectric sensors is that they are active sensors that do not require any external energy source.

## Fiber Optic Strain Gages

Fiber optic strain gages are miniature interferometers [21, 22]. Many commercially available sensors are based on the Fabry–Perot interferometer. The Fabry–Perot interferometer measures the change in the size of a very small cavity.

Fabry–Perot strain sensors (Figure 22.12) comprise a laser light source, single-mode optical fibers, a coupler (the fiber optic equivalent of a beam splitter), a cavity that senses strain, and a photodetector. Light leaves the laser diode. It passes down the fiber, through the coupler, and to the cavity. The end of the fiber is the equivalent of a partially silvered mirror. Some of the light is reflected back up the fiber and some is transmitted. The transmitted light crosses the cavity and then is reflected from the opposite end back into the fiber where it recombines with the first reflected beam. The two beams have a phase difference related to twice the cavity length. The recombined beam passes through the coupler to the photodetector. If the two reflected beams are in phase, there will be constructive interference. If the two



beams are out of phase, there will be destructive interference. The cavity is bonded to a specimen. When the specimen is strained, the cavity stretches. This results in a phase change of the cavity beam, causing a cycling between constructive and destructive interference. For a 1.3  $\mu\text{m}$  light source, each peak in output corresponds to a 650 nm gap displacement. The gap displacement divided by the gap length gives the strain. The output is continuous between peaks so that a 3 mm gage can resolve 1  $\mu\text{strain}$ .

## Birefringent Film Strain Sensing

Birefringent film strain sensors give a full field measurement of strain. A nice demonstration of this effect can be achieved with two sheets of inexpensive Polaroid film, a 6 mm thick, 25 mm  $\times$  200 mm bar of Plexiglas (polymethylmethacrylate or PMMA), and an overhead projector. Place the two Polaroid sheets at 90° to one another so that the light is blocked. Place the PMMA between the Polaroid sheets. Apply a bending moment to the bar and color fringes will appear. Birefringent materials have a different speed of light in different directions. This means that if light is polarized in a particular direction and passed through a birefringent specimen, if the fast direction is aligned with the electric field vector, the light passes through faster than if the slow direction is aligned with the electric field vector. This effect can be used to produce optical interference. In some materials, birefringence is induced by strain. The fast and slow directions correspond to the directions of principal strain, and the amount of birefringence corresponds to the magnitude of the strain. One component of the electric field vector travels through the specimen faster than the other. They emerge with a phase difference. This changes the relative amplitude and thus rotates the polarization of the light. If there is no birefringence, no light passes through the second polarizer. As the birefringence increases with strain, light passes through. As it further increases, the polarization rotation will be a full 180° and again no light will pass through. This produces a fringe that corresponds to a constant difference in principal strains. The difference in principal strains is given by Equation 22.34.

$$\varepsilon_2 - \varepsilon_1 = \frac{N\lambda}{tK} \quad (22.34)$$

where  $\varepsilon_1, \varepsilon_2$  = Principal strains

$N$  = Fringe order

$\lambda$  = Wavelength

$t$  = Specimen thickness

$K$  = Strain-optical coefficient of the photoelastic material

A similar technique can be used with a birefringent plastic film with a silvered backing laminated to the surface of a specimen. Polarized light is passed through the film; it reflects from the backing, passes back through the film, and through the second polarizer. In this case, because light passes twice through the film, the equation governing the difference in principal strains is Equation 22.35.

$$\varepsilon_2 - \varepsilon_1 = \frac{N\lambda}{2tK} \quad (22.35)$$

If the polarizers align with principal strain directions, no birefringence is observed. Rotation of both polarizers allows the principal directions to be found at various locations on the test specimen. If a full view of the fringes is desired, quarter wave plates are used (Figure 22.13). In this arrangement, light is passed through the first polarizer, resulting in plane polarization; through the quarter wave plate, resulting in circular polarization; through the test specimen, resulting in phase changes; through the second quarter wave plate to return to plane polarization; and then through the final polarizer.

The optical systems for viewing birefringence are commercially available as “Polariscopes” [23]. Optical components to construct custom systems are available from many optical components suppliers.

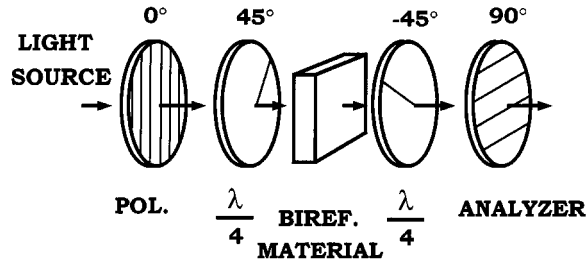


**FIGURE 22.13** A schematic of the polariscope, a system for measuring birefringence. This technique gives a full field measure of the difference in principal strains.

### Moiré Strain Sensing

Moiré interference is another technique that gives a full field measurement, but it measures displacement rather than strain. The strain field must be computed from the displacement field. This technique is based on the interference obtained when two transparent plates are covered with equally spaced stripes. If the plates are held over one another, they can be aligned so that no light will pass through or so that all light will pass through. If one of the plates is stretched, the spacing of the lines is wider on the stretched plate. Now, if one plate is placed over the other, in some regions light will pass through and in some regions it will not (Figure 22.14). The dark and light bands produced give information about the displacement field.

Moiré is defined as a series of broad dark and light patterns formed by the superposition of two regular gratings [24]. The dark or light regions are called fringes. Examples of pure extension and pure rotation are shown. In both cases, some of the light that would emerge from the first grating is obstructed by the superimposed grating. At the centers of the dark fringes, the bar of one grating covers the space of the other and no light comes through. The emergent intensity,  $I$ , is zero. Proceeding from there toward the next dark fringe, the amount of obstruction diminishes linearly and the amount of light increases linearly until the bar of one grating falls above the bar of the other. There, the maximum amount of light passes through the gratings.

Both geometric interference and optical interference are used. This discussion is restricted to geometric interference. Geometric moiré takes advantage of the interference of two gratings to determine displacements and rotations in the plane of view. In-plane moiré is typically conducted with two gratings, one applied to the specimen (specimen grating) and the other put in contact with the specimen grating (reference grating). When the specimen is strained, interference patterns or fringes occur.  $N$  is the moiré fringe order. Each fringe corresponds to an increase or decrease of specimen displacement by one grating pitch. The relationship between displacement and fringes is  $\delta = gN$ , where  $\delta$  is component of the displacement perpendicular to the reference grating lines,  $g$  is reference grating pitch, and  $N$  is the fringe order.

For convenience, a zero-order fringe is designated assuming the displacement there is zero. With the reference grating at  $0^\circ$  and  $90^\circ$ , the fringe orders  $N_x$  and  $N_y$  are obtained. The displacements in  $x$ ,  $y$  directions are then obtained from Equations 22.36 and 22.37.

$$u_x(x, y) = gN_x(x, y) \tag{22.36}$$

$$u_y(x, y) = gN_y(x, y) \tag{22.37}$$

Differentiation of Equations 22.36 and 22.37 gives the strains, Equations 22.38 through 22.40.

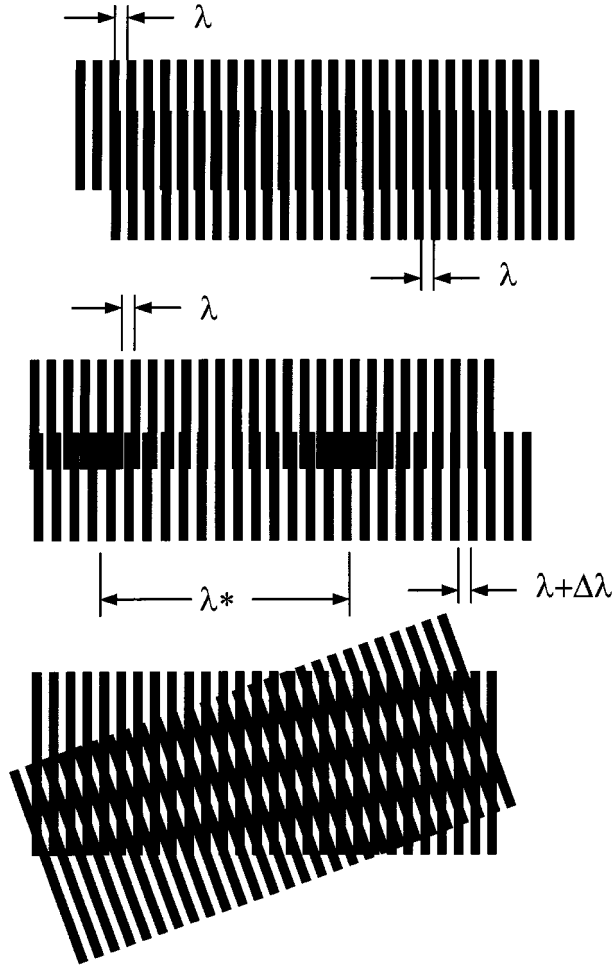


**FIGURE 22.14** A demonstration of moiré fringes formed by overlapping gratings. The fringes are the result of stretching and relative rotation of the gratings. The fringe patterns are used to determine displacement fields.

$$\epsilon_x = \frac{\partial u_x}{\partial x} = g \frac{\partial N_x}{\partial x} \quad (22.38)$$

$$\epsilon_{xy} = \frac{1}{2} \left( \frac{\partial u_y}{\partial x} + \frac{\partial u_x}{\partial y} \right) = \frac{1}{2} \left( g \frac{\partial N_y}{\partial x} + g \frac{\partial N_x}{\partial y} \right) \quad (22.39)$$

$$\epsilon_y = \frac{\partial u_y}{\partial y} = g \frac{\partial N_y}{\partial y} \quad (22.40)$$

In most cases, the sensitivity of geometric moiré is not adequate for determination of strain distributions. Strain analysis should be conducted with high-sensitivity measurement of displacement using moiré interferometry [24, 25]. Moiré interferometers are commercially available [26]. Out-of-plane measurement can be conducted with one grating (the reference grating). The reference grating is made to interfere with either its reflection or its shadow [27, 28].

## References

1. N. E. Dowling, *Mechanical Behavior of Materials*, Englewood Cliffs, NJ: Prentice-Hall, 1993, 99-108.
2. R. C. Craig, *Mechanics of Materials*, New York: John Wiley & Sons, 1996.
3. A. Vengsarkar, Fiber optic sensors: a comparative evaluation, *The Photonics Design and Applications Handbook*, 1991, 114-116.
4. H. U. Eisenhut, Force measurement on presses with piezoelectric strain transducers and their static calibration up to 5 MN, *New Industrial Applications of the Piezoelectric Measurement Principle*, July 1992, 1-16.
5. TN-501-4, Strain Gauge Temperature Effects, Measurements Group, Inc., Raleigh, NC 27611.
6. TN-509, Transverse Sensitivity Errors, Measurements Group, Inc., Raleigh, NC 27611.
7. TT-609, Soldering Techniques, Measurements Group, Inc., Raleigh, NC 27611.
8. TN-515, Strain Gage Rosettes, Measurements Group, Inc., Raleigh, NC 27611.
9. TN-08-1, Fatigue of Strain Gages, Measurements Group, Inc., Raleigh, NC 27611.
10. C. C. Perry and H. R. Lissner, *The Strain Gage Primer*, New York: McGraw-Hill, 1962.
11. J. B. Aidun and Y. M. Gupta, Analysis of Lustrangian gauge measurements of simple and nonsimple plain waves, *J. Appl. Phys.*, 69, 6998-7014, 1991.
12. Y. M. Gupta, Stress measurement using piezoresistance gauges: modeling the gauge as an elastic-plastic inclusion, *J. Appl. Phys.*, 54, 6256-6266, 1983.
13. D. Y. Chen, Y. M. Gupta, and M. H. Miles, Quasistatic experiments to determine material constants for the piezoresistance foils used in shock wave experiments, *J. Appl. Phys.*, 55, 3984, 1984.
14. C. S. Lynch, Strain compensated thin film stress gauges for stress wave measurements in the presence of lateral strain, *Rev. Sci. Instrum.*, 66(11), 1-8, 1995.
15. B-129-7 M-Line Accessories Instruction Bulletin, Measurements Group, Inc., Raleigh, NC 27611.
16. J. W. Dally, W. F. Riley, and K. G. McConnell, *Instrumentation for Engineering Measurements*, 2nd ed., New York: John Wiley & Sons, 1993.
17. J. P. Holman, *Heat Transfer*, 7th ed., New York: McGraw Hill, 1990.
18. Dynasen, Inc. 20 Arnold Pl., Goleta, CA 93117.
19. M. Dean (ed.) and R. D. Douglas (assoc. ed.), *Semiconductor and Conventional Strain Gages*, New York: Academic Press, 1962.
20. Kistler, Instruments Corp., Amhurst, NY, 14228-2171.
21. J. S. Sirkis, Unified approach to phase strain temperature models for smart structure interferometric optical fiber sensors. 1. Development, *Opt. Eng.*, 32(4), 752-761, 1993.
22. J. S. Sirkis, Unified approach to phase strain temperature models for smart structure interferometric optical fiber sensors. 2. Applications, *Optical Engineering*, 32(4), 762-773, 1993.
23. Photoelastic Division, Measurements Group, Inc., P.O. Box 27777, Raleigh, NC 27611.
24. T. Valis, D. Hogg, and R. M. Measures, Composite material embedded fiber-optic Fabry-Perot strain rosette, *SPIE*, 1370, 154-161, 1990.
25. D. Post, B. Han, and P. Lfju, *High Sensitivity Moiré*, New York: Springer-Verlag, 1994.
26. V. J. Parks, Geometric Moiré, *Handbook on Experimental Mechanics*, A. S. Kobayashi, Ed., VCH Publisher, Inc., 1993.
27. Photomechanics, Inc. 512 Princeton Dr. Vestal, NY, 13850-2912.
28. T. Y. Kao and F. P. Chiang, Family of grating techniques of slope and curvature measurements for static and dynamic flexure of plates, *Opt. Eng.*, 21, 721-742, 1982.
29. D. R. Andrews, Shadow moiré contouring of impact craters, *Opt. Eng.*, 21, 650-654, 1982.